Nanoscale

Accepted Manuscript

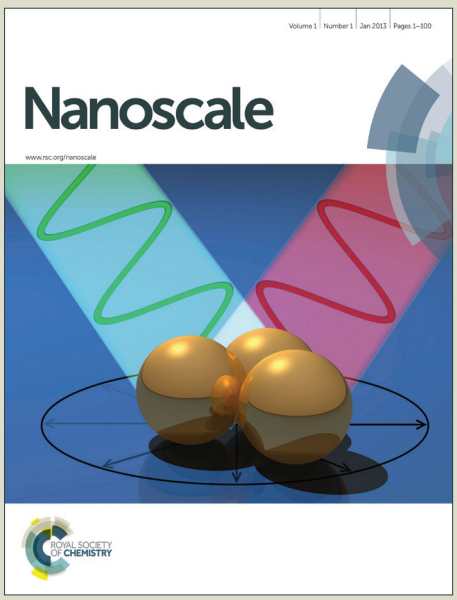

This is an *Accepted Manuscript*, which has been through the Royal Society of Chemistry peer review process and has been accepted for publication.

Accepted Manuscripts are published online shortly after acceptance, before technical editing, formatting and proof reading. Using this free service, authors can make their results available to the community, in citable form, before we publish the edited article. We will replace this *Accepted Manuscript* with the edited and formatted *Advance Article* as soon as it is available.

You can find more information about *Accepted Manuscripts* in the Information for Authors.

Please note that technical editing may introduce minor changes to the text and/or graphics, which may alter content. The journal's standard Terms & Conditions and the Ethical guidelines still apply. In no event shall the Royal Society of Chemistry be held responsible for any errors or omissions in this *Accepted Manuscript* or any consequences arising from the use of any information it contains.

ROYAL SOCIETY OF CHEMISTRY

www.rsc.org/nanoscale

Cite this: DOI: 10.1039/c0xx00000x

www.rsc.org/xxxxxx

Paper

Continuous flow purification of nanocrystal quantum dots

Duckjong Kim,[*†,§], Hye Kyung Park[†], Hyekyoung Choi[†,§], Jaehong Noh[†], Kyungnam Kim[†], and Sohee Jeong,[*†,§]

Received (in XXX, XXX) Xth XXXXXXXXX 20XX, Accepted Xth XXXXXXXXX 20XX
DOI: 10.1039/b000000x

Colloidal quantum dot (QD) purification is typically conducted via repeating precipitation-redispersion involving massive amount of organic solvents and has been the main obstacle in mass production of QDs with dependable surface properties. Our results show that the electric field apparently affects the streamline of QDs and that we could continuously collect stably dispersed QDs by using the electrophoretic purification process. The purification yield increases as the electric potential difference increases or the flow rate decreases, but reaches an asymptotic value. The yield can be further improved by raising the absolute magnitude of the mobility of QDs with the addition of solvents with high dielectric constants. The continuous purification process sheds light on industrial production of colloidal nanomaterials.

Introduction

Colloidal quantum dots are semiconducting nanocrystals whose electronic and optical characteristics are highly tunable and have a lot of applications including bio-imaging, photovoltaics, displays, lighting, etc.[1,2] Nanocrystal quantum dots (QDs) are typically synthesized in coordinating or non-coordinating solvents with large number of hydrocarbons enabling high temperature crystal growth. Unreacted precursors, excess amount of surfactants, and reaction media should be removed for any further composite fabrication and bio-functionalization of quantum dots.[3-5] Non-solvents are added to form flocculated quantum dot-aggregates. By repeating precipitation and redispersion in pure solvents, purified QDs are collected.[6] Yet simple, precipitation-redispersion is not scalable, require massive amounts of additional solvents, and more importantly, not controllable. Depending on the precursor used, size of the dots, and even morphology of the dots have a noticeable effect on the purification process.[7-9] For industrial use of QDs, large scale synthesis as well as the scalable purifications is required. Recently, it has been reported that continuous synthesis of QDs by fine tuning of the temperature and the flow rate of the fluid containing precursors could scale up the QD synthetic process.[10-12] However, purification process of QDs still remains as a batch process and the incompatibility between the continuous synthesis process and the batch type purification step has been the main obstacle in mass production of QDs. In this study, we present a continuous QD purification process based on electrophoresis. As-prepared QDs in organic solvent prepared via batch process or continuous flow process can directly applied to our electrophoretic purification set up. Further removal of surface coordinating ligands is feasible as well by controlling the electrophoretic force applied to the QDs in the microfluidic channel confirmed by nuclear magnetic resonance (NMR) analysis.

Experimental section

Cadmium oxide (Aldrich, 99.99%), Oleic acid (Alfa, 99%), Trioctylphosphine (TOP, Aldrich, 97%), 1-octadecene (ODE, Aldrich, 90%), and Selenium (Aldrich, 99.99%) were used as purchased without further purification. All manipulations were performed using the standard Schlenk line techniques. In a typical synthesis, cadmium oxide (0.0515 g), oleic acid (0.5 mL), and 1-octadecene (10 mL) was degassed in three-neck flask for 30min under vacuum. The solution was then heated for 1.5 h to 110°C. The solution turned transparent. Hereafter, the flasks were heated to 305°C at nitrogen atmosphere, and removed from the heating mantle. TOPSe (2M, 0.2 mL) was prepared by mixing Se (0.79 g) shot in trioctylphosphine (10 mL) and loaded into a 1 mL of syringe and then rapidly injected into the solution at 300°C.

We fabricated the microfluidic chip by using the standard MEMS processes (see the Supporting Information, Figure S1).

Nanoscale Accepted Manuscript

We made microchannel openings in two 400 micron thick silicon substrates by using the deep reactive-ion etching. We aligned the two silicon substrates and thermally bonded the substrates to form the H-filter structure. We deposited the chromium (30 nm) and gold (100 nm) layers functioning as the electrode on two Pyrex 7740 glass substrates and patterned the layers. We made penetrating holes through the glass substrates to form inlets and outlets of the chip by using the sand blasting. We covered the bonded silicon substrate with the glass substrates by using the anodic bonding. The electrodes on the top and bottom glass substrates face the inside of the chip.

We infused the as-prepared QD dispersions, which contain unreacted precursors and excess surfactants as impurities and the pure target solvent, which we expect our QD dispersed as a final solution, into the microfluidic chip having H-filter structure by using a syringe pump (KDS210, KD Scientific) and applied electric potential difference to the electrodes of the chip by using a DC power supply (6575A, Agilent) to generate the electrophoretic movement of QDs in the microfluidic chip. The flow rate of the target solvent stream is three times as large as that of the as-prepared QD stream to avoid diffusional mixing of unwanted impurities. The electric potential difference applied to the electrodes spaced 800 μm apart ranges from 0 to 100 V.

The absorption spectra were obtained using a UV/Vis spectrophotometer (Shimadzu, UV3600) for samples dissolved in hexane. Photoluminescence (PL) spectra were recorded using a Horiba Fluorolog spectrometer at room temperature using a xenon lamp as the excitation source. The quantum yield was measured by absolute quantum yield (QY) measurement system (C-9920-02, Hamamatsu, Japan).

Electron micrograph images of QDs on a carbon-coated Cu mesh grid were obtained using Tecnai F30 Super-Twin (FEI Co., Hillsboro, OR, USA; operated by Yun-Chang Park, KAIST NanoFab). The particle size distribution was estimated from transmission electron microscopy images using the software GATAN Digital Micrograph 3.9.0 (GATAN Inc., Warrendale, PA, USA). Attenuated Total Reflectance Fourier transform infrared (ATR FT-IR) spectra were obtained on a Thermo Scientific Nicolet 6700 spectrometer equipped with a smart miracle accessory. NMR data were collected using an AVANCE III 600 spectrometer (^{1}H frequency of 600 MHz).

Results and discussion

Electrophoresis is the particle movement relative to a fluid under an electric field. Since the electrophoretic behaviour of particles is relatively well understood and highly controllable, it has been explored widely to manipulate nanoparticles. Specifically, Alivisatos group and others attempted to separate DNA conjugated QDs using gel electrophoresis for obtaining surface charge controlled QDs.[11] More recently, Bass et al., reported that the QDs can be purified in large scale using electrophoresis.[13-14] They immersed electrodes in QD dispersed organic solution and collected purified QDs by applying high voltage (typically 500 V), which shows the possibility of less operator-dependent and more environmentally friendly

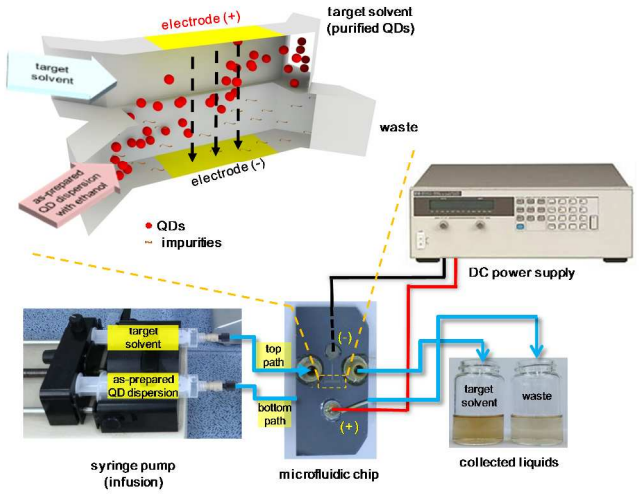

Figure 1 Quantum dot electrophoretic purification setup.

nanoparticle purification, yet the batch type implementation exposes limit in the process scale up. Here, we used the electrophoretic movement of QDs in a laminar flow through a microchannel and demonstrated continuous purification of QDs as shown in Figure 1. Organic solvent resistant silicon was patterned to form the microchannels.[15] We then tested the fabricated chip by using the experimental set up shown in Figure 1. CdSe QDs used in this study were prepared via the hot injection method (see the Supporting Information, Figure S2).[16] For the as-prepared QD dispersed in hexane, the electrophoretic mobility of QDs is very small (~ 0 cm^2/Vs) due to the low dielectric constant (1.89) of the solvent. Since the mobility is proportional to the dielectric constant,[9] we added ethanol with relatively high dielectric constant (24.3) to the QD dispersion to increase the mobility. When the ratio of ethanol to QD dispersion reaches to 2:8, the absolute magnitude of the mobility increases to 5.7×10^{-5} cm^2/Vs.

Figure 2A shows that the electric field apparently affects the streamline of QDs. QDs are distinctly found in the target solvent stream only when the electric field is applied to the laminar flow in the microchannel. Collected target solvents which contain purified QDs and wastes were further analyzed via UV/Vis/NIR absorption spectroscopy for the quantification. Without the electrophoresis, no signature absorption feature from QD was detected (Figure 2B) which supports that QDs did not move to the stream of the target solvent without the electric field. The position of the first exciton peak is 608 nm regardless of the ethanol addition and the electrophoretic purification indicating that the purification process did not affect the charge state of QD.[17] Furthermore, purified QDs showed an excellent colloidal stability even after one month monitored via retained flat baseline below the band edge energy from UV-Vis measurements.

More QDs in the stream of the as-prepared QD dispersion move to the stream of the target solvent as the electric potential difference increases. (Figure 2B) The purification yield is defined as the ratio of the amount of QDs in the target solvent to the total amount of QDs. The amount of QDs in the dispersion is determined by the QD concentration and the volume of the

Nanoscale Accepted Manuscript

This journal is © The Royal Society of Chemistry [year]

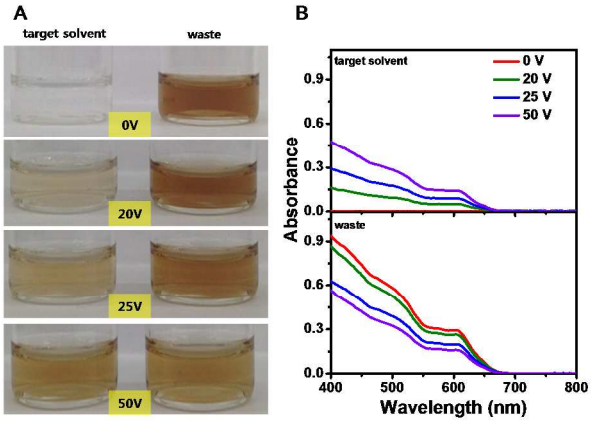

Figure 2 Electrophoretic purification of QDs. (A) Collected liquids from outlets of microfluidic chip. (B) UV/VIS absorbance spectra of collected liquids.

dispersion. We estimated the QD concentration of the dispersion from the intensity of the first exciton peak (I) in the absorption spectra divided by the extinction coefficient (ε) of the QDs and the optical path length (b) in the spectroscopy. We got the amount of QDs by multiplying the QD concentration and the dispersion volume (A). Finally, we obtained the purification yield as follows:

$$(\text{purification yield}) = \frac{(\text{IA})_{\text{target}}/_{\epsilon b}}{(\text{IA})_{\text{target}}/_{\epsilon b} + (\text{IA})_{\text{waste}}/_{\epsilon b}} = \frac{(\text{IA})_{\text{target}}}{(\text{IA})_{\text{target}} + (\text{IA})_{\text{waste}}} \quad (1)$$

where the subscripts 'target' and 'waste' represent the properties of the dispersion from the outlet for the target solvent stream and that from the other outlet for the waste stream, respectively. The extinction coefficient and the path length are same regardless of where the dispersion was from. To improve the purification yield, i.e., to move more QDs to the stream of the target solvent, we need to 1) raise the electric potential across the electrodes to increase the electrophoretic velocity or 2) reduce the flow rate of the QD dispersion to increase the retention time of QDs in the area exposed to the electric field.

Purification yield increases with the electric potential difference and reaches a plateau when the electric potential exceeds a certain value as shown in Figure 3. The yield limit is 49 %. The fact that the yield no longer increases with the electric potential difference when the potential exceeds the critical potential indicates that there might be a critical electrophoretic mobility under which the electrophoretic QD movement does not occur. When the flow rate in the microfluidic chip changes, just the retention time for which the QDs are exposed to the electric field changes. Hence, the critical potential at which the purification yield reaches the plateau would be proportional to the flow rate of the solvent because the electrophoretic velocity of QDs proportional to the electric potential difference should increase with the flow

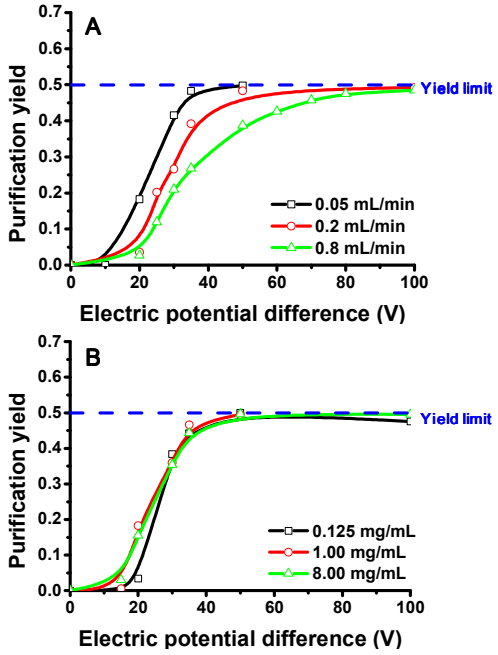

Figure 3 Purification yield monitored with electric potential difference increase for various (A) total flow rates through microfluidic chip (0.05, 0.2, and 0.8 mL/min) and (B) QD concentrations (0.125, 1.0, 8.00 mg/mL). The lines are just guide for eyes.

velocity to move QDs to the target solvent during the retention time. When the electric potential is smaller than the critical value, the purification yield would decrease as the flow rate increases for the same electric potential difference as shown in Figure 3A. We also checked the effect of the QD concentration on the purification result. (Figure 3B) The change in the purification yield due to the QD concentration change is negligible. The yield obviously increases as the electric potential difference increases or the flow rate decreases but finally reaches an asymptotic value. If we assume that there is no critical mobility for the electrophoretic movement, we can roughly estimate the required magnitude of the mobility (μ_e) for QD movement to the target solvent stream from the cross-sectional dimensions of the microchannel (D: the distance between the electrodes, W: the microchannel width), the length of the electrode (L), electrical potential difference across the electrodes (V) and the total liquid flow rate (Q). To move the QDs to the target stream during the QDs are exposed to the electric field, the multiplication of the electrophoretic velocity ($\mu_e V/D$) and the retention time of the QDs exposed to the electric field (LDW/Q) should be comparable to the distance between the electrodes.

$$\mu_e \frac{V}{D} \frac{L}{Q/_{DW}} \sim D \quad (2)$$

From equation (2), we can find the required mobility to move the QDs to the target stream for the specified dimensions, the total liquid flow rate and the electric potential difference as follows:

Nanoscale Accepted Manuscript

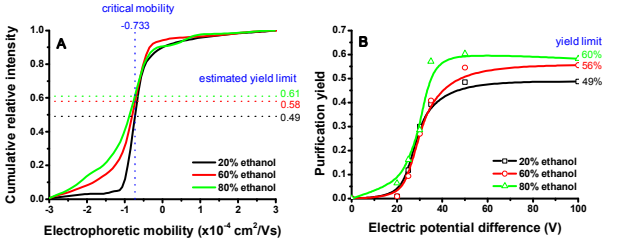

Figure 4 Effect of ethanol content on (A) cumulative distribution of electrophoretic mobility of QDs and (B) purification yield (lines: guide for eyes).

$$\mu_e \sim \frac{QD}{VLW} \qquad (3)$$

QDs having the electrophoretic mobility equal to or higher than the required mobility can move to the target stream. Therefore, if the required mobility decreases, more QDs can move to the target stream. Equation (3) indicates that the required mobility decreases – in other words, the purification yield increases for specified QDs – as the flow rate decreases or the electric potential difference increases as discussed before without the assumption of the critical mobility. However, the experimental results show that the yield could not exceed the limit regardless of the operation conditions as shown in Figure 3. Moreover, when we increase the electric potential difference over the critical potential, the amount of QDs remained in the waste stream does not decrease with the increase in the electric field strength. Hence, there must be a critical mobility for the electrophoretic movement of QDs. Figure 4A shows the cumulative distributions of the mobility for various ethanol contents. When the ethanol content is 20 %, because the asymptotic value of the yield is 49 %, QDs with mobility in the top 49 % would move to the target solvent stream and we can estimate the critical mobility for the purification by searching for the mobility where the cumulative distribution function is 0.49. The absolute magnitude of the critical mobility is found to be 7.3×10^{-5} cm^2/Vs. Figure 4A shows that, when ethanol content increase to 80 %, 61 % of QDs have the mobility higher than the critical value. Hence, we can expect the yield of 61 % based on the electrophoretic mobility distribution of QDs. The experimental data for the yield limit shown in Figure 4B matches well with the value estimated based on the mobility distribution shown in Figure 4A. This confirms that the yield is dominated by the distribution of the electrophoretic mobility of QDs. Our results show that the purification yield limitingly depends on the electric field or the retention time of QDs for a specified solvent and that the yield limit can be improved by raising the absolute magnitude of the mobility of QDs with the addition of a solvent with high dielectric constant.

We also investigated emission properties of QDs before and after the electrophoretic purification. Figure 5A shows that the relative PL intensity of QDs does not depend on the electrical potential difference in the process of the purification and the elapsed time after the purification. Figure 5B shows that the position and the width of the emission peak do not change due to

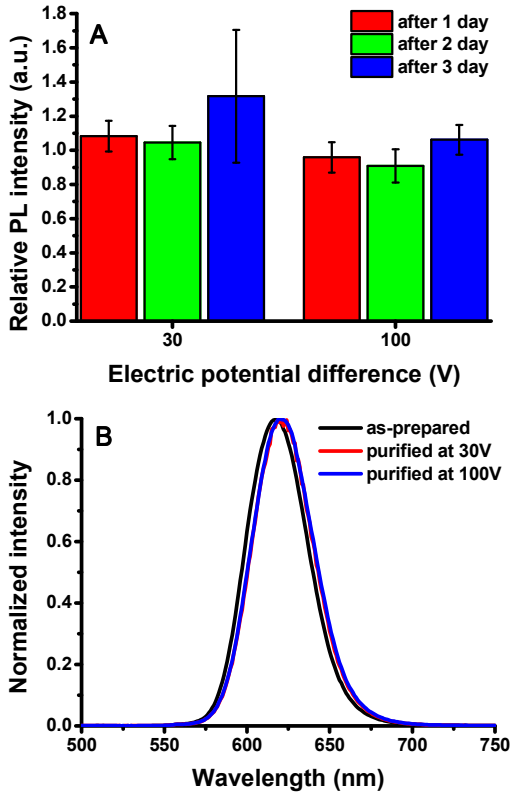

Figure 5 Emission properties of QDs purified at 30 V and 100 V. (A) Relative photoluminescence(PL) intensity of purified QDs over time, 1, 2, and 3 days, respectively. (B) Photoluminescence spectra.

the electrophoretic purification, neither. Our results indicate that the emission properties of QDs are well maintained in the process of the purification. As previously confirmed by absorption spectroscopy (Figure 2), PL measurement proves that the electophoretic purification do not affect the trap states of CdSe as well as the electronic level.

ATR-FTIR spectroscopy has long been used to monitor and quantify the ligands on QD surfaces.[18] We analyzed the amount of Cd(oleate)$_2$ using ATR-FTIR to confirm the efficient removal of Cd(oleate)$_2$ via our electrophoretic purification scheme. (Figure 6) QD capped with oleate in hexane before and after the electrophoretic purification at 70 V with same optical density at 400 nm in absorption spectra were investigated. Figure 6 shows the survey spectra of CdSe QDs. The peaks around 3000 cm^{-1} indicate C-H stretch signal and the peaks around 1500 cm^{-1} display COO stretch signal.[19] We focus on the region around 1500 cm^{-1} to calculate the amount of Cd(oleate)$_2$ in Figure 6(inset). 15 percent decrease in the amount of Cd(oleate)$_2$ after the electrophoretic purification at 70 V was seen, which is comparable to the result of the traditional precipitation-redispersion method. (Figure S3) As we confirmed that our electrophoretic purification do not alter the electronic structure of CdSe QDs in this study, we further studied the surface chemistry

Nanoscale Accepted Manuscript

This journal is © The Royal Society of Chemistry [year]

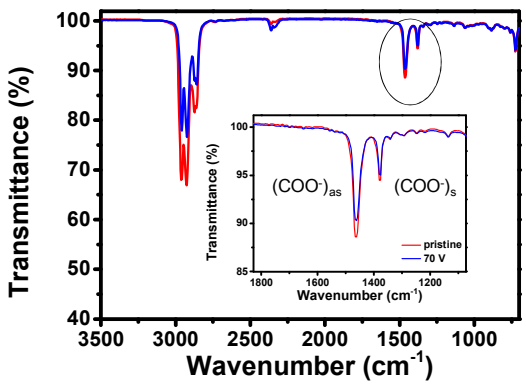

Figure 6 ATR-FTIR spectra of CdSe QDs capped with oleate before (red line) and after (blue line) electrophoretic purification at 70 V and the inset shows COO^- stretch region.

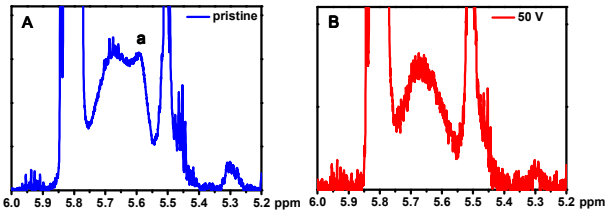

Figure 7 ^{1}H NMR spectra of CdSe QDs before (A) and after (B) electrophoretic purification at 50 V.

of QDs after the purification. Surface chemistry of QDs has been investigated extensively using X-ray photoelectron spectroscopy which allows chemical analysis of surface of nanomaterials. Yet highly sensitive thereby effective in studying the surface of nanocrystals, only solid state samples can be studied.[20,21] Using ^{1}H solution NMR measurement, bound oleate to CdSe QDs, unreacted precursors like $Cd(oleate)_2$, and excess surfactants can be distinguished in solution.[22,23] Figure 7 indicates the ^{1}H solution NMR spectra of CdSe QDs capped with oleate in benzene-d, before and after the electrophoretic purification at 50 V, respectively. We focus the peak corresponding to vinyl group of oleate between 5.2 and 6.0 ppm in NMR spectra. In both spectra, peaks around 5.8 ppm which correspond to protons on the alkene in remaining octadecene used as solvent during synthesis and the sharp peak at 5.5 ppm is assigned to freely unbound oleate to surface of CdSe QDs.[24,25] The broad resonances in the region between 5.55 and 5.75 ppm indicate the protons of tightly bound oleate ligands. Before the electrophoretic purification, we find the broad shoulder peak 'a' next to sharp free oleate ligand peak at 5.6 ppm which corresponds to the CdSe monomer or cluster remain on the surface of QDs.[22] Monomers or clusters in CdSe QD solution have been known to disturb well-ordered array in the film, consequently, lead to adversely affected electrical properties when we fabricate a device.[26] Interestingly, after the purification, peak 'a' was removed completely. Therefore we suggest that our electrophoretic purification is effective not only removing unreacted precursors in solution but also effective in detaching loosely bound clusters which could impair device performances afterwards.

To use the proposed process in industrial site, scale up of the process is crucial. The electric field magnitude is one of the key parameters determining the purification yield and it depends on the applied potential difference and the distance between the electrodes. Hence, when we just increase the dimensions of the flow path except for the distance between the electrodes, we could increase the handling capacity without reducing the yield. Parallelization of the process could be another way for the scale up. In addition, since the purification yield does not depend on the QD concentration, use of highly concentrated QD dispersion would be helpful in increasing the purification capacity.

Conclusions

We have presented a continuous QD purification process based on electrophoresis. Our results show that the electric field apparently affects the streamline of QDs and that we could continuously collect stably dispersed QDs by using the electrophoretic purification process. The purification yield increases as the electric potential difference increases or the flow rate decreases, but reaches an asymptotic value. The yield can be further improved by raising the absolute magnitude of the mobility of QDs with the addition of solvents with high dielectric constants. Electrophoretic purification could effectively remove the bound precursors on QD surfaces which is beneficial for optoelectric applications. We expect that the continuous purification process could be scaled up by relatively simple ways such as the flow path enlargement and parallelization. In addition, use of highly concentrated QD dispersion would increase the purification capacity. The present work shows a new possibility of QD mass production and would be a cornerstone of industrial use of QDs.

Acknowledgements

This work was supported by the government funding research program (NK181C) funded by Korea Research Council for Industrial Science & Technology (ISTK) and the Global Frontier R&D Program by the Center for Multiscale Energy Systems funded by the National Research Foundation under the Ministry of Science, ICT, and Future, Korea (2011-0031566)

Notes and references

[†]*Department of Nano Mechanics, Korea Institute of Machinery and Materials (KIMM), Daejeon 305-343, South Korea.*
[§]*Korea University of Science and Technology (UST), 206 Gajeong-ro, Daejeon 305-350, South Korea.*
Fax: +82-42-868-7884; Tel: +82-42-868-7121; E-mail: dkim@kimm.re.kr, sjeong@kimm.re.kr

Electronic Supplementary Information (ESI) available: Additional figures on the microfluidic chip fabrication, QD size analysis, and the effect of

Nanoscale Accepted Manuscript

the solution environment (dilution) on removal of ligands. See DOI: 10.1039/b000000x/

1 A. P. Alivisatos, W. Gu, and C. Larabell, *Annu. Rev. Biomed. Eng.*, 2010, **7**, 55-76.
2 A. Nozik, *Physica E,* 2002, **14**, 115-120.
3 S. Jeong, M. Achermann, J. Nanda, S. Ivanov, V. I. Klimov, and J. A. Hollingsworth*, J. Am. Chem. Soc.,* 2005**, 127**, 10126-10127.
4 W. C. Chan and S. Nie, *Science,* 1998, **281**, 2016-2018.
5 H. T. Uyeda, I. L. Medintz, J. K. Jaiswal, S. M. Simon, and H. Mattoussi, *J. Am. Chem. Soc.,* 2005*,* **127**, 3870-3878.
6 C. Murray, D. J. Norris, and M. G. Bawendi, *J. Am. Chem. Soc.,*1993, **115**, 8706-8715.
7 H. Zhang, J. S. Son, J. Jang, J.-S. Lee, W.-L. Ong, J. A. Malen, and D. V. Talapin, *ACS nano,* 2013 **7**, 10296-10306
8 B. Dabbousi, J. Rodriguez-Viejo, F. V. Mikulec, J. Heine, H. Mattoussi, R. Ober, K. Jensen, and M. Bawendi, *J. Phys. Chem. B*, 1997, **101**, 9463-9475.
9 C. Murray, C. Kagan, and M. Bawendi, *Science,* 1995, **270**, 1335-1338.
10 J. Baek, P. M. Allen, M. G. Bawendi, and K. F. Jensen, *Angew. Chem.,* 2011**, 123**, 653-656.
11 K. Kim, S. Jeong, J. Y. Woo, and C.-S. Han, *Nanotechnology*, 2012, **23**, 065602.
12 J. Pan, A. a. O. El-Ballouli, L. Rollny, O. Voznyy, V. M. Burlakov, A. Goriely, E. H. Sargent, and O. M. Bakr, *ACS nano*, 2013, **7**, 10158-10166.
13 A. Fu, C. M. Micheel, J. Cha, H. Chang, H. Yang, and A. P. Alivisatos, *J. Am. Chem. Soc.,*2004, **126**, 10832-10833.
14 J. D. Bass, et al., Angew. Chem. Int. Ed., 2011 **50**, 6538-6542.
15 H. Lorenz, M. Despont, N. Fahrni, N. LaBianca, P. Renaud, and P. Vettiger*, J. Micromech. Microeng.,* 1997, **7**, 121.
16 C. R. Bullen and P. Mulvaney, *Nano Lett.*, 2004, **4**, 2303-2307.
17 M. Shim and P. Guyot-Sionnest, *Nature,* 2000, **407**, 981-983.
18 A. G. Young, N. Al-Salim, D. P. Green, and A. J. McQuillan, *Langmuir*, 2008, **24**, 3841-3849.
19 J. M. Luther, M. Law, Q. Song, C. L. Perkins, M. C. Beard, and A. J. Nozik, *ACS nano*, 2008, **2**, 271-280.
20 H. Choi, J.-H. Ko, Y.-H. Kim, and S. Jeong, *J. Am. Chem. Soc.,* 2013, **135**, 5278-5281.
21 J. Y. Woo, J.-H. Ko, J. H. Song, K. Kim, H. Choi, Y.-H. Kim, D. C. Lee, and S. Jeong, *J. Am. Chem. Soc.,* 2014, **135**, 8883-8886.
22 Z. Hens and J. C. Martins, *Chem. Mater*., 2013, **25**, 1211-1221.
23 N. C. Anderson, M. P. Hendricks, J. J. Choi, and J. S. Owen, *J. Am. Chem. Soc.,* 2013, **135**, 18536-18548.
24 A. Hassinen, I. Moreels, K. De Nolf, P. F. Smet, J. C. Martins, and Z. Hens, *J. Am. Chem. Soc.,*2012, **134**, 20705-20712.
25 S. J. Oh, N. E. Berry, J.-H. Choi, E. A. Gaulding, T. Paik, S.-H. Hong, C. B. Murray, and C. R. Kagan, *ACS nano* 2013, **7**, 2413-2421
26 L. C. Cass, M. Malicki, and E. A. Weiss,. *Anal. chem.* 2013, **85**, 6974-6979.

Textual Abstract:

Nanocrystal quantum dots are continuously purified by moving them to the impurity-free target solvent stream.

Graphical Abstract:

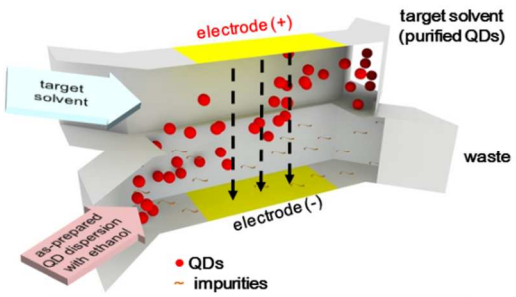

Nanoscale Accepted Manuscript

This journal is © The Royal Society of Chemistry [year]